Acta Biochim Biophys Sin (2009): 379–388 | © The Author 2009. Published by ABBS Editorial Office in association with Oxford University Press on behalf of the Institute of Biochemistry and Cell Biology, Shanghai Institutes for Biological Sciences, Chinese Academy of Sciences. DOI: 10.1093/abbs/gmp017.
Advance Access Publication 24 March 2009

Characterization of the putative tryptophan synthase β-subunit from *Mycobacterium tuberculosis*

Hongbo Shen[1†], Yanping Yang[1†], Feifei Wang[1], Ying Zhang[2], Naihao Ye[3], Shengfeng Xu[1*], and Honghai Wang[1*]

[1]State Key Laboratory of Genetic Engineering, School of Life Sciences, Fudan University, Shanghai 200433, China
[2]Department of Molecular Microbiology and Immunology, Bloomberg School of Public Health, Room E2037, Johns Hopkins University, 615 North Wolfe Street, Baltimore, MD 21205, USA
[3]Yellow Sea Fisheries Research Institute, Chinese Academy of Fishery Sciences, Qingdao 266071, China
*Correspondence address. Tel: +86-21-65643777; Fax: +86-21-65648376; E-mail: hhwang@fudan.edu.cn (H.W.); Tel: +86-21-65643777; Fax: +86-21-65648376; E-mail: xushengfeng2001@hotmail.com (S.X.)
†These authors contributed equally to this work.

The increasing emergence of drug-resistant tuberculosis (TB) poses a serious threat to the control of this disease. It is in urgent need to develop new TB drugs. Tryptophan biosynthetic pathway plays an important role in the growth and replication of *Mycobacterium tuberculosis* (*Mtb*). The β-subunit of tryptophan synthase (TrpB) catalyzes the last step of the tryptophan biosynthetic pathway, and it might be a potential target for TB drug design. In this study, we overexpressed, purified, and characterized the putative TrpB-encoding gene *Rv1612* in *Mtb* H37Rv. Results showed that *Mtb* His-TrpB optimal enzymatic activity is at pH 7.8 with 0.15 M Na^+ or 0.18 M Mg^{2+} at 37°C. Structure analysis indicated that *Mtb* TrpB exhibited a typical β/α barrel structure. The amino acid residues believed to interact with the enzyme cofactor pyridoxal-5′-phosphate were predicted by homology modeling and structure alignment. The role of these residues in catalytic activity of the *Mtb* His-TrpB was confirmed by site-directed mutagenesis. These results provided reassuring structural information for drug design based on TrpB.

Keywords tryptophan synthase; *Mycobacterium tuberculosis*; enzyme activity; active site; site-directed mutation

Received: December 10, 2008 Accepted: March 3, 2009

Introduction

Tuberculosis (TB), caused by *Mycobacterium tuberculosis* (*Mtb*), is one of the most dangerous bacterial human pathogens with significant morbidity and mortality worldwide [1]. Every year, there are more than eight million new TB cases and three million deaths [2]. HIV infection is contributing to the increasing number of TB cases among immunocompromised individuals [3]. In addition, the increasing emergence of multiple drug-resistant TB (MDR-TB) and extensively drug-resistant TB poses a serious threat to the control of this disease. Furthermore, it is reported that 79% of MDR-TB cases are 'super strains' resistant to at least three of the four main drugs used in TB treatment [4]. Thus, there is an urgent need to develop new TB drugs for the treatment of drug-resistant TB.

It is well known that the current TB drugs target a restricted set of microbial processes. Our search for new enzyme targets to combat *Mtb* has focused on the tryptophan biosynthetic pathway. It was reported that auxotroph of *Mtb*, which is knockout in the tryptophan biosynthetic pathway, showed attenuation in the ability to infect mice, even in immunodeficient mice [5]. It indicated that the amino acid might be unavailable for uptake by the bacterium *in vivo* [6]. Additionally, tryptophan biosynthesis is absent in mammals but is a general metabolic pathway in prokaryotes, which makes the enzymes of this biosynthetic pathway effective targets for new anti-TB agents.

The tryptophan synthase (TSase; EC 4.2.1.20) catalyzes the last two reactions in the biosynthesis of tryptophan [7]. This enzyme has an $\alpha_2\beta_2$ structure in all bacterial species [8,9]. A complex of α- and β-subunits catalyze the αβ reaction [10]. The monomeric α-subunit alone catalyzes the α reaction and the dimeric β_2-subunit

catalyzes the β reaction, which is the last step of tryptophan biosynthesis. The detail is shown in the following:

α reaction: indole-3-glycerol phosphate $\rightleftharpoons$ indole + D–glyceraldehyde-3-phosphate

β reaction: indole + L–serine$\rightarrow$L–tryptophan + H_2O

$\alpha\beta$ reaction: indole-3-glycerol phosphate + L–serine$\rightarrow$D–glyceraldehyde-3-phosphate + L–tryptophan

It is easy to conclude that inhibition of β-subunit catalytic activity will cause the failure of tryptophan biosynthesis. And that, TSases as pyridoxal-5′-phosphate (PLP)-dependent enzymes are widely recognized as drug targets [11]. So, it means that tryptophan synthase β-subunit (TrpB) from *Mtb* might be a potential target for the design of new anti-TB drugs. Hence, a detailed biochemical and biophysical characterization of *Mtb* TrpB is necessary for effective drug design.

In this study, we reported the biochemical characterization of the recombinant *Mtb* TrpB. The active sites of *Mtb* TrpB were predicted through structure alignment and confirmed by site-directed mutagenesis.

Materials and Methods

Reagents

All chemicals were purchased from Sigma (St Louis, MO, USA) unless otherwise specified. All restriction endonuclease, polymerase, and ligase were purchased from New England Biolabs (Beijing, China). Bacterial genomic DNA extraction, plasmid extraction, and gel extraction kits were bought from Watson Biotechnologies (Shanghai, China). Nickel–nitrilotriacetic acid (Ni–NTA) His-binding resin and columns were obtained from Qiagen (Hilden, Germany). The pET30a plasmid was obtained from Novagen (Gibbstown, NJ, USA).

Bacterial strains and culture conditions

Mycobacterium tuberculosis H37Rv was provided by Shanghai Pulmonary Hospital (Shanghai, China). The other plasmids and strains used in this study were all purchased from Novagen.

Mtb H37Rv was cultured in 7H9 Middlebrook broth with 10% (v/v) oleic acid–albumin–dextrose complex (BBL, Cockeysville, MD, USA) and 2% glycerol at 37°C. *Escherichia coli* DH5α and BL21 (DE3), used for cloning and expression, respectively, were propagated in Luria–Bertani (LB) medium or on agar with 25 μg/ml of kanamycin at 37°C.

Construction of the fusion expression plasmid pET30a-TrpB

The *TrpB* gene (*Rv1612*) [12], encoding the TrpB enzyme, was amplified using *Mtb* H37Rv genomic DNA as a template by PCR with the following primers: 5′-AAAGGATCCATGAGTGCTGCCATCGCC-3′ and 5′-ATAAAGCTTCAGTCGTTGCCCAGCAAGC-3′, which contained *Bam*HI and *Hin*dIII restriction sites, respectively (underlined). The expected 1248 bp (1233 + 15 bp) fragment was obtained by PCR amplification. The resulting PCR product was digested with *Bam*HI and *Hin*dIII restriction enzymes and extracted with a gel extraction kit. The fragment was ligated to the pET30a vector, which was already digested with *Bam*HI and *Hin*dIII. The ligation mixture was transformed into DH5α, and the recombinant plasmid, named pET30a-TrpB, was identified by restriction digestion with *Bam*HI and *Hin*dIII.

Expression and purification of TrpB protein

The recombinant pET30a-TrpB plasmid was transformed into the *E. coli* BL21(DE3) to produce the recombinant TrpB protein with His-tag in the N-terminus (named His-TrpB). Transformed cells were cultured at 37°C in LB medium supplemented with kanamycin (50 μg/ml) until the optical density at 600 nm (OD_{600}) reached 0.4 − 0.6. Isopropyl-D-thiogalactopyranoside (IPTG) was added to the bacterial culture with a final concentration of 0.5 mM at 20°C for 12 h.

Bacteria were harvested by centrifugation (5650 rpm, 15 minutes, 4 °C, rotor No. 5.5, Hima CR22E) and then were lysed by sonication. The resulting lysate was centrifuged at 10700 rpm (rotor No. 8.8, Hima CR22E) for 1 h at 4°C. The supernatant was used for purification using immobilized metal affinity chromatography according to the manufacturer's protocol. The homogeneity of fractions was analyzed by SDS–PAGE. The purified His-TrpB was dialyzed against 5 mM Tris–HCl buffer (pH 7.9) and stored at −80°C. To identify the catalytic activity of *Mtb* TrpB with sufficient TrpA enzymes in mixtures, the *TrpA* gene of *Mtb* was also cloned, expressed, and purified using similar methods as described for TrpB. The primers for cloning the *TrpA* gene are shown as follows: 5′-AAAAAGCTTATGGTGGCGGTGGAACAGAGC-3′ and 5′-AAACTCGAGTCATGCGGACATCCCTAGTCG-3′, containing *Hin*dIII and *Xho*I restriction sites, respectively (underlined).

Chemical cross-linking of recombinant protein

The recombinant His-TrpB was chemically cross-linked by a modified procedure [13] as follows: 0.05 mg protein was dissolved in 20 ml of KH_2PO_4/K_2HPO_4 buffer (50 mM; pH 6.0), and 50% glutaraldehyde (0.83 ml) was added to a final concentration of 2%. The reaction was incubated at room temperature for 22 h. Then, 0.5 ml of freshly prepared 2 M $NaBH_4$/0.1 M NaOH was added to quench the reaction. The protein samples were immediately prepared for SDS–PAGE analysis.

Circular dichroism measurements

To determine the secondary structure elements of the recombinant protein, we carried out far-UV spectroscopic studies using a JASCO-715 spectrometer (Tokyo, Japan) equipped with RTE bath/circulator (NESLAB RTE-111; NESLAB, Tokyo, Japan). After a 30-min N_2 purge, the spectra were recorded from 190 to 300 nm with a protein concentration of 0.2 mg/ml (pH 7.9). The reported spectrum was the average of five scans, which were normalized for buffer control. Secondary structure parameters were estimated by the computer program PROSEC by Chang *et al.* [14].

High-performance liquid chromatography analysis

Purified recombinant protein was subjected to a Reverse Phase Column (C-18 column; Agilent, Santa Clara, CA, USA) at a flow rate of 1 ml/min. After washing with 0.1% trifluoroacetic acid (TFA), the protein was eluted with an increasing linear gradient of 80% isopropanol in 0.085% TFA.

Mass spectrometry analysis

The homogeneity of protein fractions was assessed by mass spectrometry. Samples were analyzed on a Voyager-DE-PRO mass spectrometer (Applied Biosystems, Foster City, CA, USA) by matrix-assisted laser desorption ionization time-of-flight (MALDI-TOF) with the following parameters: grid, 95%; delayed time, 1100 ns; and low mass gate, 1000 Da. The matrix was sinapinic acid, and mass spectra were obtained in the delayed extraction, positive ion, and linear mode with an accelerating voltage of 25 kV.

Determination of enzyme activity

The TSase enzyme activity was assayed by a modification of the Dettwiler and Kirschner method [15]. The reaction mixture (500 μl) included 0.1 M Tris–HCl buffer (pH 7.8), 0.18 M NaCl, 0.2 mM indole, 0.04 M L-serine, 0.01 mM pyridoxal phosphate, and more than 3-fold TrpA protein in amount. The TrpB protein was mixed with the reaction mixture before the reaction occurred. The β reaction was followed measuring the increase in absorbance due to the conversion of indole to L-Trp. The reaction was measured by the change in absorption at 290 nm with a JASCO U-530 UV/VIS spectrophotometer at 37°C using a JASCO PSC-498S Temp controller.

The optimal reaction temperature of *Mtb* TrpB was determined by comparison of the enzymatic activities at different temperatures. The effects of Na^+ and Mg^{2+} on TrpB activities were determined through the addition of different amount of NaCl or $MgCl_2$ in the assay mixture.

Determination of thermal stability of TrpB

Thermal stability of TrpB was studied by incubating the purified recombinant protein at different temperatures for 15 min. The samples were transferred to an ice water bath immediately for at least 10 min before determination of the residual enzymatic activity and were compared with the unheated controls.

Kinetic properties of TrpB and its mutants

Kinetic parameters of purified *Mtb* His-TrpB and its mutants were determined. The Michaelis–Menten constant (K_m) was determined under different concentrations of substrates indole and L-serine. K_m and V_{max} values were plotted using Lineweaver–Burk plots. K_{cat} values of wild His-TrpB and mutants were calculated.

Removal of His tag fused to recombinant TrpB in the N-terminus

The His tag fused to N-terminus of His-TrpB was cleaved by incubation of the purified His-TrpB protein with enterokinase at 6°C for 8 h. Then the enterokinase was removed according to the kit's protocol. The TrpB protein without His tag was isolated from the cleaved protein mixture by affinity capture on Ni–NTA His-binding agarose with shaking (100 rpm on a rotary shaker) at 4°C for 20 min. The flow-through was collected and then dialyzed against 5 mM Tris–HCl buffer (pH 8.0). The enzyme activities of His-TrpB and TrpB without His tag were compared at the same conditions.

Homology modeling

The 3D structure of *Mtb* TrpB was generated with the homology modeling using the Modeller 8.0 software [16]. The best model was identified through model

evaluation in MODELLER objective function values. The template used in this experiment is the B chain of the crystal structure of TrpB from *Salmonella typhimurium* at 1.4 Å resolution (PDB code 1QOP) with amino sequence identity of 56.0% to the *Mtb* TrpB.

Site-directed mutagenesis

The structure of *Mtb* TrpB was aligned with that of 1QOP, and the PLP-binding site in *Mtb* TrpB was predicted. Residues surrounding PLP within 5 Å distance in *Mtb* TrpB structure were selected for mutation analysis, except for the glycine residues at 246, 247, 248, 317, and 391 sites. Site-directed mutagenesis was performed according to the protocol described in the QuikChange Site-Directed Mutagenesis Kit (Stratagene, Santa Clara, CA, USA) using the mutagenic primers listed in **Table 1**. The wild-type *TrpB* recombinant plasmid constructed above was used as the parental plasmid for the construction of mutagenic *TrpB*. The sequences of the mutant gene of interest were verified by DNA sequencing. Purified plasmids were transformed into *E. coli* BL21(DE3) for expression of all mutant fusion proteins. The conditions of protein purification and enzyme active assay were the same as those of the wild-type TrpB enzyme as described above.

Results

Expression and purification of *Mtb* TrpB

To express the *TrpB* gene of *Mtb* H37Rv in *E. coli*, we cloned this gene using PCR and ligated it into the pET30a plasmid to express the TrpB protein fused with the 6× His tag. **Figure 1(A)** shows that the recombinant TrpB protein was overexpressed in *E. coli* BL21(DE3) (lane 1) and most proteins were present in the lysate supernatant (lane 2). After washing with 30 mM imidazole to elute other proteins (lane 3), we obtained the purified target protein which displayed a single band in SDS–PAGE of molecular weight (MW) ∼50 kDa (lane 4). Mass spectrometry analysis [**Fig. 1(B)**] showed that the exact MW of this protein is 50,224.0 Da, which is nearly equal to the sum of the TrpB theoretical MW 43,286.6 Da plus the MW 6992.9 Da of amino acids in vector. These results suggest that we have succeeded in the expression of the recombinant *Mtb* TrpB.

Cross-linking of *Mtb* TrpB

It has been reported that TrpB enzymes can catalyze the β reaction as dimers [17,18]. To determine whether *Mtb* TrpB could assemble in polymer form, we carried out cross-linking experiment of recombinant TrpB proteins. Results of SDS–PAGE analysis showed that there was an obvious protein band with MW of ∼100 kDa in the lane of cross-linked sample and that almost all *Mtb* TrpB formed dimers [**Fig. 1(C)**, lane 2]. This implies that *Mtb* TrpB may also be functional as a dimer as in other bacteria, such as *S. typhimurium* [19] and *Thermotoga maritime* [20].

Kinetic characterization of *Mtb* TrpB

Without an available enzyme assay for *Mtb* TrpB, we referred to the protocols used for other bacterial TrpB proteins [21] and optimized the enzyme assay conditions for *Mtb* TrpB. It has been reported that the subunit interface of TSase mediates the 10- to 100-fold activation of the α and β activity in the $\alpha_2\beta_2$ complex with respect to the isolated subunits [22,23]. Because of this, a reaction mixture of *Mtb* TrpB contained more than 3-fold *Mtb* TrpA protein. We compared the relative activities of *Mtb* TrpB proteins at different temperatures. Results showed that the enzyme activity reached a maximum at 37°C [**Fig. 2(A)**]. It is consistent with the optimal growth temperature of *Mtb*.

The effect of cations on the activity of *Mtb* TrpB was evaluated in the presence of different concentrations of Na^+ and Mg^{2+}. This enzyme required either Na^+ or Mg^{2+} to reach its maximal activity as shown in **Fig. 2(B)** and **(C)**. The optimal concentration of Na^+ was 0.15 M, whereas the optimal concentration of Mg^{2+} was 0.18 M. These results are consistent with other TrpBs [20]. Thus, the optimal enzyme assay condition was 0.1 M Tris–HCl buffer (pH 7.8) containing 0.15 M Na^+ or 0.18 M Mg^{2+} as well as the substrates and coenzyme in a reaction at 37°C.

Heat stability of *Mtb* TrpB

To test the stability of His-TrpB against irreversible inactivation by heat, samples of recombinant proteins were incubated at different temperatures, and the residual catalytic activities were measured at the optimal conditions mentioned above. Results showed that the enzyme activity decreased significantly when the temperature was >40°C [**Fig. 2(D)**]. The activity of enzyme incubated at 80°C was <10% of that incubated at 10°C. These results suggested that high temperature greatly reduced the activity of *Mtb* TrpB.

Substrate specificity of *Mtb* TrpB

To determine the substrate specificity of indole and L-serine for *Mtb* His-TrpB, we measured the reaction rate

Table 1 The mutagenic primers used in site-directed mutagenesis

Mutation type	Mutagenic primers (5′→3′)	
Ser99Ala	Up	AACCATACTGGT**GCT**CACAAGATCAAC
	Down	GTTGATCTTGTG**AGC**ACCAGTATGGTT
His100Ala	Up	CATACTGGTTCT**GCC**AAGATCAACAAC
	Down	GTTGTTGATCTT**GGC**AGAACCAGTATG
Gln128Ala	Up	ACCGGTGCCGGC**GCG**CACGGGGTCGCC
	Down	GGCGACCCGTG**CGC**GCCGGCACCGGA
Thr204Ala	Up	TACTGCTTTGGT**GCT**GCGGCCGGACCG
	Down	CGGTCCGGCCGC**AGC**ACCAAAGCAGTA
Ser249Ala	Up	GTTGGTGGCGGG**GCC**AATGCCATTGGT
	Down	ACCAATGGCATT**GGC**CCCGCCACCAAC
Asn250Ala	Up	GGTGGCGGGTCC**GCT**GCCATTGGTATT
	Down	AATACCAATGGC**AGC**GGACCCGCCACC
Glu364Ala	Up	ATCCCGGCTATT**GAA**TCCGCGCACGCG
	Down	CGCGTGCGCGGA**TTC**AATAGCCGGGAT
Ser390Ala	Up	GTGGTGAACCTG**GCG**GGACGTGGCGAC
	Down	GTCGCCACGTCC**CGC**CAGGTTCACCAC

The bold and underlined nucleotides are the sites to introduce mutations in DNA molecule.

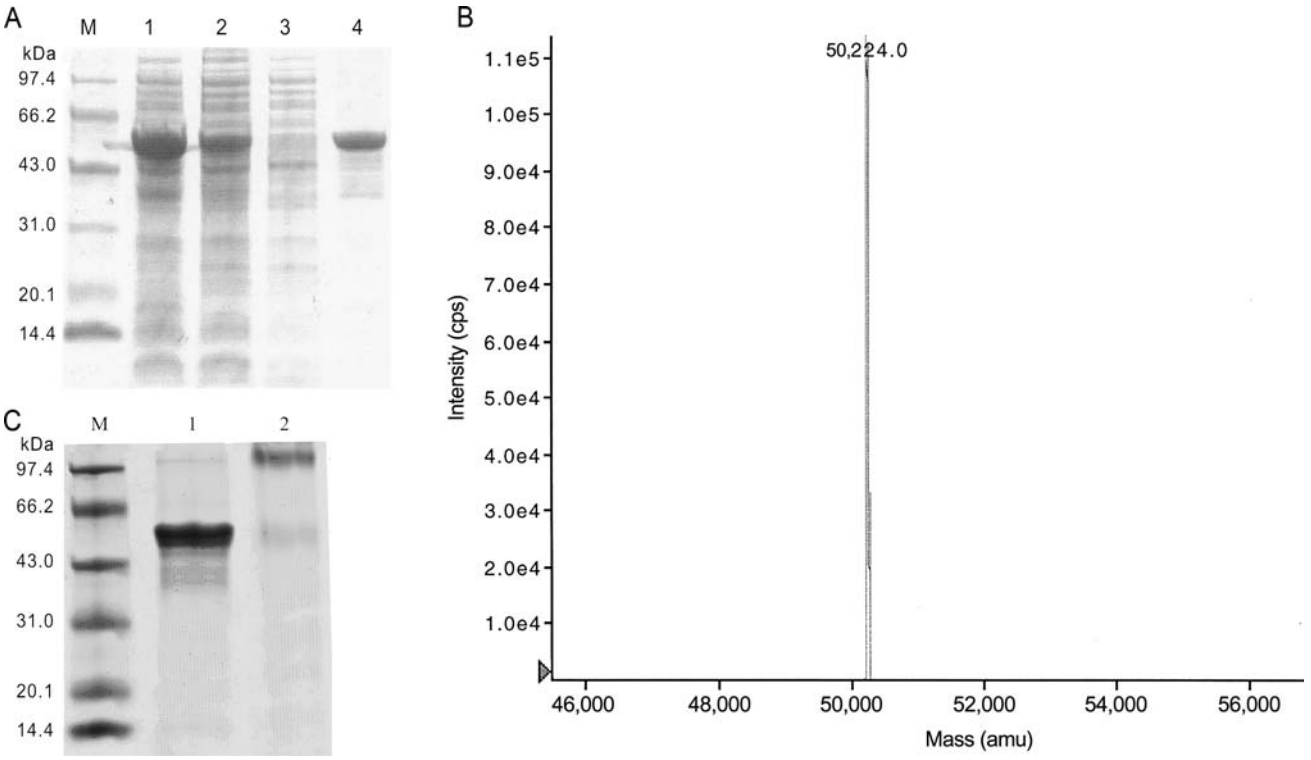

Fig. 1 Purification of *Mtb* His-TrpB protein (**A**) Purification of *Mtb* His-TrpB. Lane M, MW maker; lane 1, induced whole-cell lysate; lane 2, sonicated supernatant of *E. coli* (induced with IPTG); lane 3, fraction eluted with wash buffer containing 30 mM imidazole; lane 4, purified *Mtb* His-TrpB. (**B**) Mass-fingerprinting analysis of *Mtb* His-TrpB by MALDI-TOF. (**C**) Identification of the cross-linked recombinant TrpB of *Mtb*. Lane M, MW marker; lane 1, recombinant TrpB monomer; lane 2, His-TrpB protein dimer (upper strip).

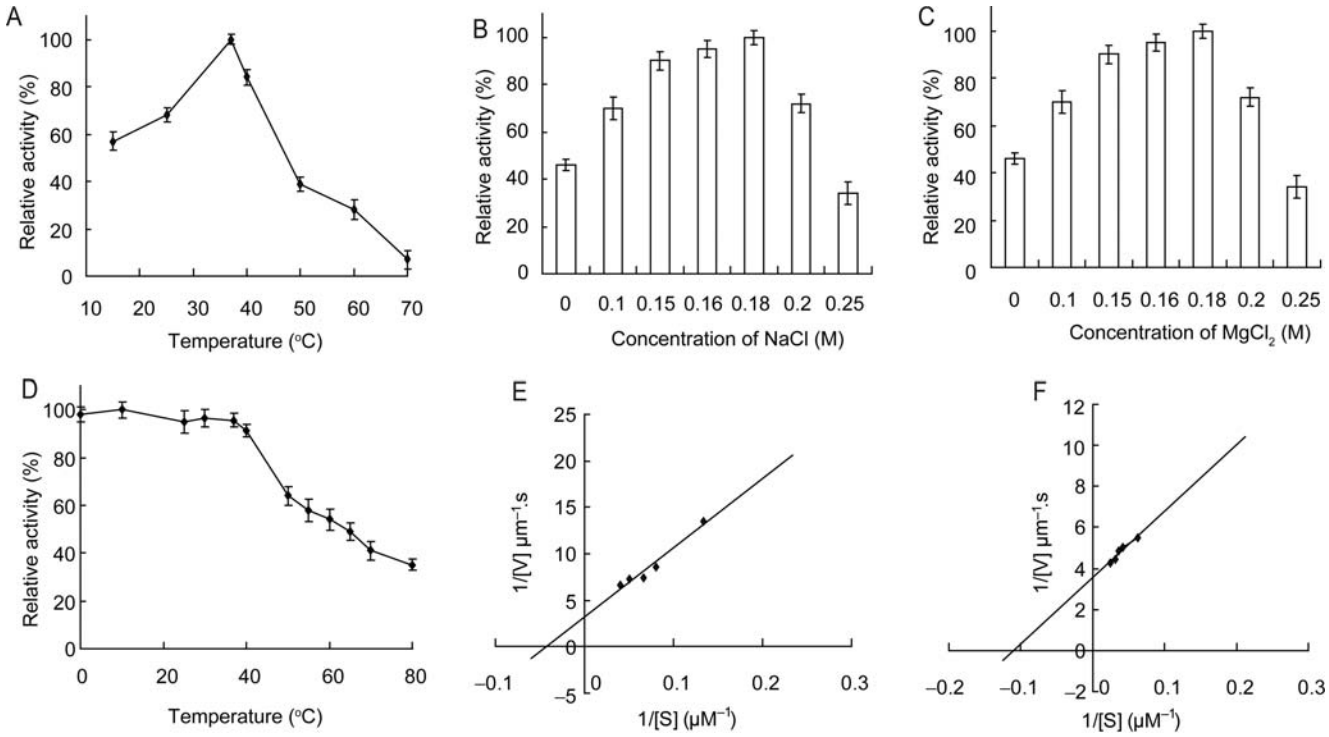

Fig. 2 Enzymatic properties of recombinant *Mtb* TrpB protein (**A**) The comparison of His-TrpB activities at different temperatures. (**B**) Effect of Na^+ concentration on His-TrpB activity. (**C**) Effect of Mg^{2+} concentration on His-TrpB activity. (**D**) Comparison of His-TrpB stability at different temperatures. (**E**) The dependence on initial velocity on indole concentration. (**F**) The dependence on initial velocity on L-serine concentration. All the values on every point in (E) and (F) are the average of five values.

of the β reaction at the optimal conditions with different substrate concentrations. The K_m values were calculated by the plot of reciprocal of reaction rate plotted vs. reciprocal of substrate concentrations. The K_m value of indole for TrpB enzyme was 0.288 mM [**Fig. 2(E)**] and 0.178 mM for L-serine [**Fig. 2(F)**]. The K_{cat} values of TrpB enzyme were also evaluated to be 70.287 s^{-1} for indole and 48.206 s^{-1} for L-serine.

Effect of His tag on TrpB catalytic activity

Figure 3(A) showed that the isolated target protein was ~7 kDa less than His-TrpB, which implied that TrpB without His tag (lane 1) was obtained by enterokinase treatment of the purified His-TrpB. We compared the relative activities of His-TrpB with TrpB without His tag at different reactive temperatures. Results indicated that both His-TrpB and TrpB were maximally active at 37°C, and there was no obvious influence of His tag on TrpB activity [**Fig. 3(B)**].

Structure analysis of *Mtb* TrpB

Recombinant TrpB protein was subjected to far-UV CD measurements. The temperature was set at 37°C to be consistent with the optimal growth temperature of *Mtb* strains. The CD spectrum of the purified protein showed a maximum in ellipticity at 190 nm and two minimums at 210 and 217 nm [**Fig. 4(A)**]. These results indicated that the recombinant TrpB protein, which was composed by α-helices and β-sheets, was actually folded. Furthermore, the 3D structure of *Mtb* TrpB generated by homology modeling [**Fig. 4(B)**] suggested that it was a β/α barrel structure composed by α-helices, and β-sheets with random loops connecting them.

Determination of the binding site of PLP in *Mtb* TrpB

We aligned structure of the *Mtb* TrpB enzyme and the complex structure of *S. typhimurium* TrpB with PLP and then analyzed the residues required for the binding of PLP in two enzymes. There are 13 residues surrounding PLP within 5 Å distance in *Mtb* TrpB [**Fig. 5(A)**] and *S. typhimurium* TrpB [**Fig. 5(B)**], respectively. Eight of the 13 residues surrounding PLP were mutated to alanine with side chain of methyl group except the glycine residues at 246, 247, 248, 317, and 391 sites. The enzyme activities of mutants were assayed under the same

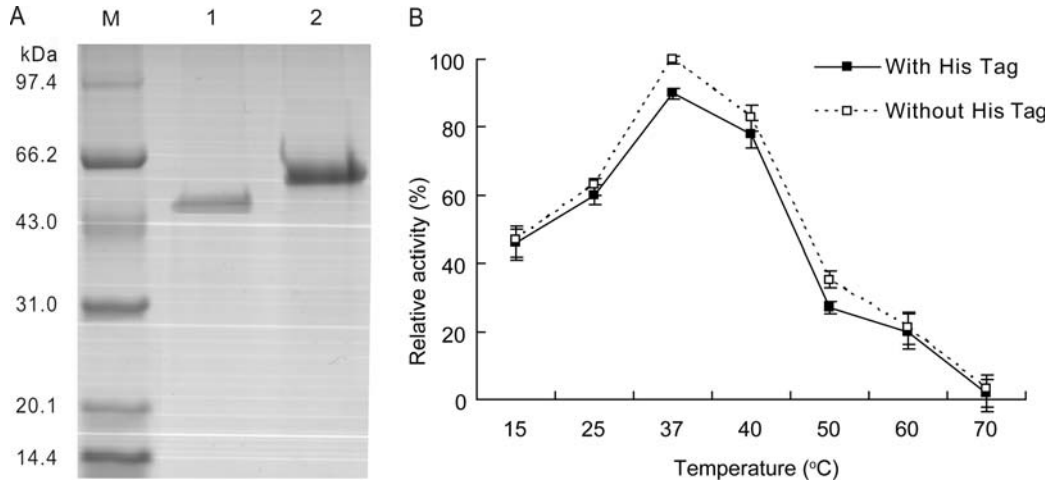

Fig. 3 Effect of His tag on TrpB catalytic activity (**A**) Purification of TrpB after removal of N-terminal fusion partner by enterokinase treatment. Lane M, MW marker; lane 1, the recombinant His-TrpB protein; lane 2, purified TrpB protein without His tag. Proteins were visualized with Coomassie Brilliant Blue staining. (**B**) Effect of reactive temperature on TrpB catalytic activity. Solid lines are the results of recombinant His-TrpB. Dashed lines are the results of TrpB without His tag. Bars represent ± SD.

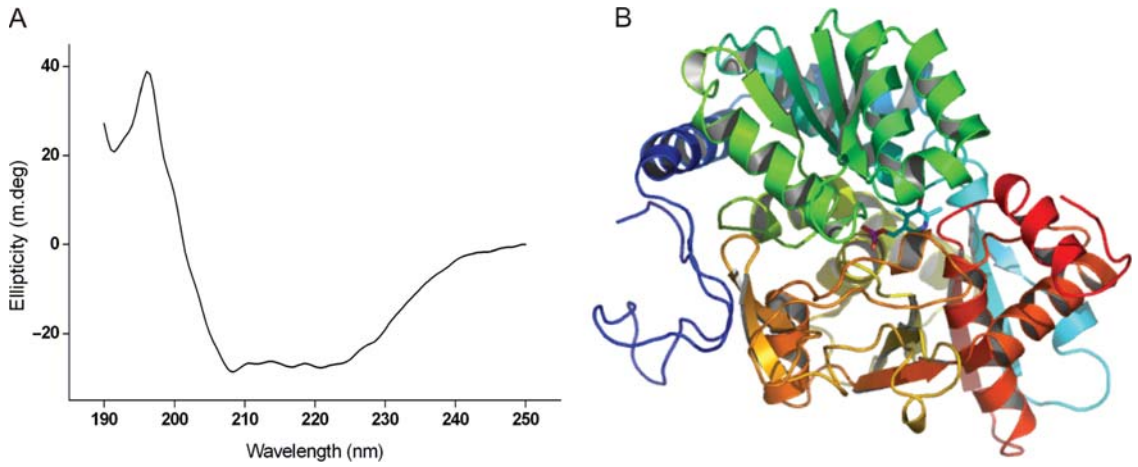

Fig. 4 Structural analysis of *Mtb* TrpB protein (**A**) Circular dichroism spectrum of purified His-TrpB protein. Percentage of secondary structure elements of His-TrpB was α-helix, 30.9%; β-sheet, 22.1%; β-turn, 19.7%; and random coil, 27.3%. Proteins were measured in 2 mM Tris−HCl, pH 7.9, at 37°C. (**B**) The predicted structure of *Mtb* TrpB protein. The molecule in the center is PLP.

conditions. Results demonstrated that the K_m values of indole and L-serine increased remarkably, and K_{cat} values for indole and L-serine decreased significantly (**Table 2**). These results might imply that the catalytic activities of these mutants decrease. Especially, the mutations at His100 and Glu364 which make the K_m values of indole and L-serine all increase >10 folds. And the K_{cat} values of these mutants for indole and L-serine decrease ~28 and 24 folds, respectively. Other mutations at Ser99, Asn250, and Ser390 also decrease the enzyme activities obviously. These results showed that most of these residues were important for enzyme catalysis of *Mtb* TrpB.

Sequence alignment showed that there were 11 of the 13 PLP-binding residues conserved within two sequences [**Fig. 5(C)**]. It implied that there might be similar binding modes of enzyme cofactor PLP in *Mtb* TrpB and *S. typhimurium* TrpB. For example, the mutation at Glu364 in *Mtb* TrpB would increase the K_m values of L-serine by 22.488 folds, and this residue was corresponding to Glu350 in *S. typhimurium* TrpB enzyme. The later was revealed to play a functional role

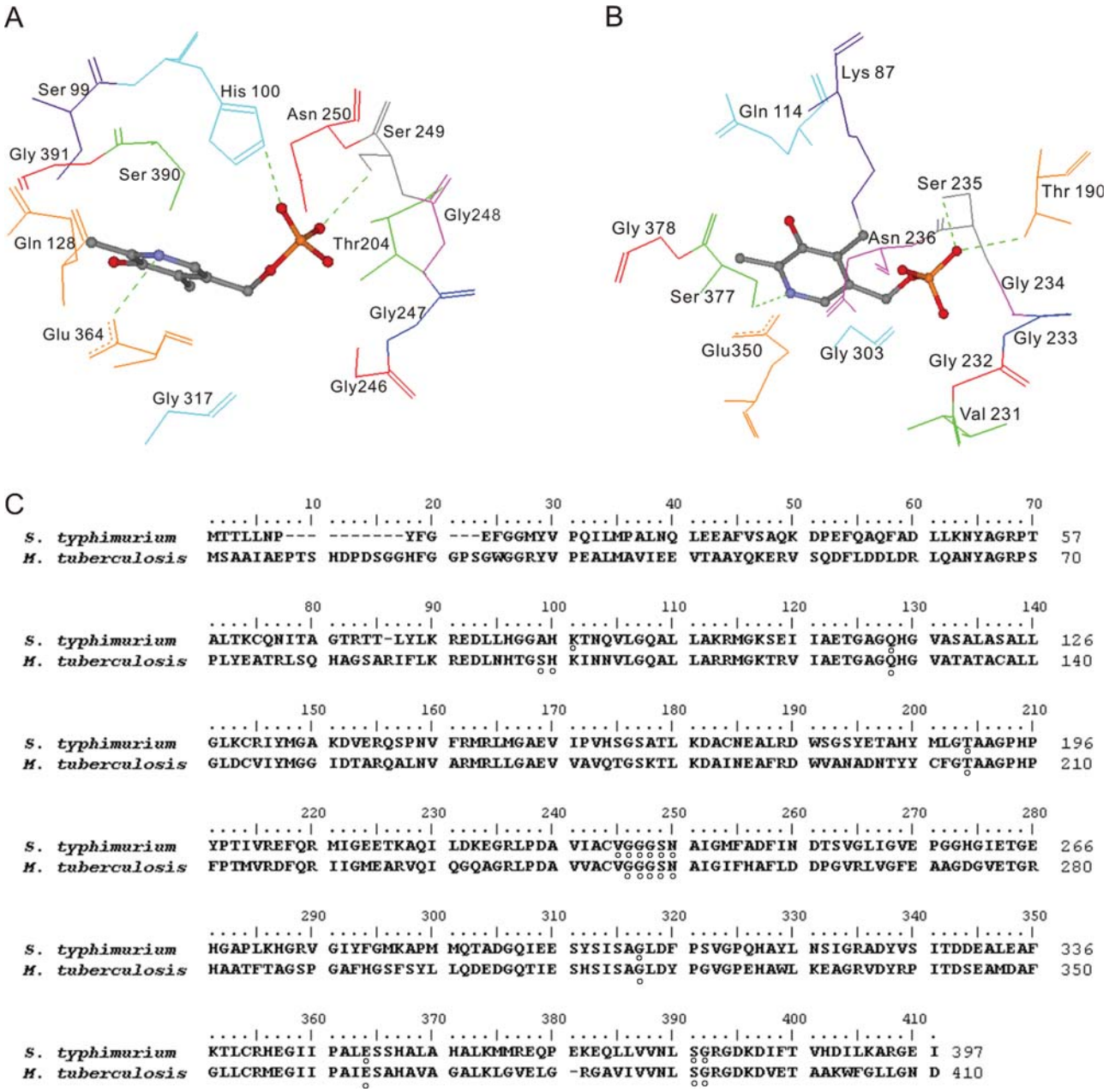

Fig. 5 Comparison of the binding sites of enzyme cofactor PLP to *Mtb* TrpB and *S. typhimurium* TrpB (**A**) The residues within 5 Å around PLP in *Mtb* TrpB. (**B**) The residues within 5 Å around PLP in *S. typhimurium* TrpB. Dashed lines (green) in (A) and (B) represent the hydrogen bonds. PLP is presented in balls and sticks in (A) and (B). (**C**) Sequence alignment of TrpB proteins of *Mtb* and *S. typhimurium*. Star represents the residues within 5 Å around PLP in *S. typhimurium* TrpB; and circle represents the residues within 5 Å around PLP in *Mtb* TrpB.

in enzyme catalysis and facilitate the β-elimination of the weak hydroxyl leaving group of L-serine [24].

Discussion

It was reported that the TSase enzymes in bacteria, such as *Chlamydia trachomatis*, are effective drug targets [25,26]. In this paper, we have cloned, expressed, purified, and characterized the TrpB of *Mtb*. Through structure alignment of this protein with its template, the PLP-binding site of *Mtb* TrpB was predicted and validated by the site-directed mutagenesis. These studies will provide to drug designers the reassuring information on the validity of the enzyme structure for developing inhibitors.

Table 2 The K_m and K_{cat} values of mutant enzymes

Name	Mutation type	Parameters for indole			Parameters for L-serine		
		K_m (mM)	K_m(Mx[a])/K_m(wild)	K_{cat} (s^{-1})	K_m (mM)	K_m(Mx[a])/K_m(wild)	K_{cat} (s^{-1})
Wild	—	0.288 ± 0.013	1	70.287 ± 2.154	0.178 ± 0.0085	1	48.206 ± 1.426
M1	Ser99Ala	2.342 ± 0.09	8.132	21.139 ± 0.857	1.683 ± 0.05	9.455	13.218 ± 0.54
M2	His100Ala	4.471 ± 0.17	15.524	2.531 ± 0.053	15.798 ± 0.39	88.753	1.987 ± 0.063
M3	Gln128Ala	0.997 ± 0.04	3.462	68.432 ± 2.04	1.052 ± 0.02	5.910	21.472 ± 1.005
M4	Thr204Ala	1.013 ± 0.03	3.517	50.649 ± 1.498	0.983 ± 0.047	5.522	16.348 ± 0.5
M5	Ser249Ala	1.485 ± 0.06	5.858	26.842 ± 1.003	1.235 ± 0.039	6.938	10.689 ± 0.448
M6	Asn250Ala	2.860 ± 0.13	9.931	40.178 ± 0.98	1.850 ± 0.078	10.393	7.106 ± 0.347
M7	Gln364Ala	2.906 ± 0.09	10.090	6.427 ± 0.136	4.0029 ± 0.16	22.488	3.462 ± 0.154
M8	Ser390Ala	2.083 ± 0.1	7.233	34.728 ± 1.95	1.9115 ± 0.078	10.739	20.483 ± 1.165

[a]Mx: M1, M2, . . ., M8.

Virtual high-throughput screening based on protein structure is a useful tool in inhibitor discovery. For example, we identified a ligand of ATB107 to have anti-mycobacterial activity *in vitro* against *Mtb* strains [27] through virtual screening based on the indole-3-glycerol phosphate synthase (IGPS) structure of *Mtb* H37Rv combining evaluation of biology experiments. The IGPS structure was constructed using homology modeling, and it was optimized through molecular dynamics simulations to make the side chains place correctly. With this approach, it is promising to get potent drug-like compounds based on the TrpB structure.

It is well known that the PLP-binding site is the region where the β reaction occurs [28]. Here, indole is converted to tryptophan in the presence of L-serine [29]. To identify β reaction site of *Mtb* TrpB, we aligned structure of the *Mtb* TrpB enzyme and the complex structure of *S. typhimurium* TrpB with PLP. Then, we analyzed the residues required for the binding of PLP in two enzymes. Mutation results showed that most of these residues were important for enzyme catalysis of *Mtb* TrpB. Results also showed that mutations in most of the residues increased the K_m value of L-serine more obviously than that of indole. It means that the mutations at these residues might mainly affect the Stage I of β reaction, where L-serine reacts with the enzyme-bound PLP cofactor. However, they could also affect the Stage II of β reaction for the Km value of indole, which mainly takes part in the Stage II of β reaction, also increased [29]. Mutations of two residues of His100 and Ser99 in *Mtb* TrpB decreased the activity of enzyme obviously, which did not belong to the binding sites of PLP in *S. typhimurium* TrpB. And that, there were also two residues of Lys87 and Val231 in *S. typhimurium* TrpB that did not belong to the binding sites of PLP in *Mtb* TrpB, though they were conserved in *Mtb* TrpB. There are many reports showing that Lys87 is an essential catalytic residue and it can form covalent bond with PLP [19,21,30]. But the distance between this residue and PLP was >5 Å in *Mtb* TrpB structure. And it seems difficult for them to form covalent bond. Whereas, residue of His100 in *Mtb* TrpB (according to His86 in *S. typhimurium* TrpB) is adjacent to Lys87 of *S. typhimurium* TrpB in amino acid sequence, and the mutation at this residue has increased the K_m value of L-serine by 88.753 folds. So, this residue, as well as Lys87 of *S. typhimurium* TrpB, might play important roles in the binding of PLP. Further work must be done to analyze the residues not only involved in PLP-binding sites but also in other catalysis-related sites.

Moreover, it has been reported that TSase is a complex composed of two α and two β-subunits in bacteria [19,31,32]. Through chemical cross-linking experiments, we have shown that *Mtb* TrpB can easily form a dimer. Further functional and structural studies of these two enzymes will also help to understand allosteric regulation, intersubunit communication, and the mechanisms underlying catalysis.

Acknowledgement

We thank Dana Emmert (Purdue University, IN, USA) for revising the manuscript and giving us many helpful suggestions.

Funding

This work was supported by the grants from the National Natural Science Foundation of China

(30570406) and the Shanghai Postdoctoral Scientific Program (06R214114).

References

1 Anon. Global tuberculosis control. WHO report 2002. World Health Organization, Geneva, Switzerland, 2002: 181.
2 Dye C, Scheele S, Dolin P, Pathania V and Raviglione MC. Consensus statement. Global burden of tuberculosis: estimated incidence, prevalence, and mortality by country. WHO Global Surveillance and Monitoring Project. JAMA 1999, 282: 677–686.
3 Raviglione MC, Snider DE and Kochi A. Global epidemiology of tuberculosis. Morbidity and mortality of a worldwide epidemic. J Am Med Assoc 1995, 273: 220–226.
4 World Health Organization. Anti-tuberculosis drug resistance in the world. Third Global Report. 2004.
5 Smith DA, Parish T, Stoker NG and Bancroft GJ. Characterization of auxotrophic mutants of *Mycobacterium tuberculosis* and their potential as vaccine candidates. Infect Immun 2001, 69: 1142–1150.
6 Lee CE, Goodfellow C, Javid-Majd F, Baker EN and Lott JS. The crystal structure of TrpD, a metabolic enzyme essential for lung colonization by *Mycobacterium tuberculosis*, in complex with its substrate phosphoribosylpyrophosphate. J Mol Biol 2006, 355: 784–797.
7 Pouwels P and Van RJ. *In vitro* synthesis of enzymes of the tryptophan operon of *Escherichia coli*. Proc Natl Acad Sci USA 1972, 69: 1786–1790.
8 Yanofsky C. Using studies on tryptophan metabolism to answer basic biological questions. J Biol Chem 2003, 278: 10859–10878.
9 Truffa-Bachi P and Cohen G. Amino acid metabolism. Annu Rev Biochem 1973, 42: 113–134.
10 Aksoy S, Squires CL and Squires C. Translational coupling of the *trpB* and *trpA* genes in the *Escherichia coli* tryptophan operon. J Bacteriol 1984, 157: 363–367.
11 Amadasi A, Bertoldi M, Contestabile R, Bettati S, Cellini B, Salvo MLd and Borri-Voltattorni C, *et al*. Pyridoxal 5′-phosphate enzymes as targets for therapeutic agents. Curr Med Chem 2007, 14: 1291–1324.
12 Cole ST, Brosch R, Parkhill J, Garnier T, Churcher C, Harris D and Gordon SV, *et al*. Deciphering the biology of *Mycobacterium tuberculosis* from the complete genome sequence. Nature 1998, 393: 537–544.
13 Hurle M, Matthews C, Cohen F, Kuntz I, Toumadje A and Johnson WJ. Prediction of the tertiary structure of the α-subunit of tryptophan synthase. Proteins 1987, 2: 210–224.
14 Chang C, Wu C and Yang J. Circular dichroic analysis of protein conformation: inclusion of the beta-turns. Anal Biochem 1978, 91: 13–31.
15 Dettwiler M and Kirschner K. Tryptophan synthase from *Saccharomyces cerevisiae* is a dimer of two polypeptide chains of Mr 76000 each. Eur J Biochem 1979, 102: 159–165.
16 Marti-Renom MA, Stuart A, Fiser A, Sánchez R, Melo F and Sali A. Comparative protein structure modeling of genes and genomes. Annu Rev Biophys Biomol Struct 2000, 29: 291–325.
17 Miles E. Tryptophan synthetase : structure, function, and subunit interaction. Adv Enzymol 1979, 49: 127–186.
18 Miles E. The tryptophan synthase $\alpha_2\beta_2$ complex. Cleavage of a flexible loop in the α subunit alters allosteric properties. J Biol Chem 1991, 266: 10715–10718.
19 Rhee S, Parris KD, Hyde CC, Ahmed SA, Miles EW and Davies DR. Crystal structures of a mutant (βK87T) tryptophan synthase $\alpha_2\beta_2$ complex with ligands bound to the active sites of the α- and β-subunits reveal ligand-induced conformational changes. Biochemistry 1997, 36: 7664–7680.
20 Hettwer S and Sterner R. A novel tryptophan synthase β-subunit from the hyperthermophile *Thermotoga maritime*. J Biol Chem 2002, 277: 8194–8201.
21 Lu Z, Nagata S, McPhie P and Milese EW. Lysine 87 in the β subunit of tryptophan synthase that forms an internal aldimine with pyridoxal phosphate serves critical roles in transimination, catalysis, and product release. J Biol Chem 1993, 268: 8727–8734.
22 Leopoldseder S, Hettwer S and Sterner R. Evolution of multi-enzyme complexes: the case of tryptophan synthase. Biochemistry 2006, 45: 14111–14119.
23 Hyde CC and Miles EW. The tryptophan synthase multienzyme complex: exploring structure-function relationships with X-ray crystallography and mutagenesis. Nat Biotech 1990, 8: 27–32.
24 KayasthaS AM, Sawaj Y, Nagatan S and Miles EW. Site-directed mutagenesis of the β subunit of tryptophan synthase from *Salmonella typhimurium*, role of active site Glutamic acid 350. J Biol Chem 1991, 266: 7618–7625.
25 Stoll SW, Kansra S and Elder JT. Metalloproteinases stimulate ErbB-dependent ERK signaling in human skin organ culture. J Biol Chem 2002, 277: 26839–26845.
26 Caldwell H, Wood H, Crane D, Bailey R, Jones R, Mabey D and Maclean I, *et al*. Polymorphisms in *Chlamydia trachomatis* tryptophan synthase genes differentiate between genital and ocular isolates. J Clin Invest 2003, 111: 1757–1769.
27 Shen H, Wang F, Zhang Y, Huang Q, Xu S, Hu H and Yue J, *et al*. A novel inhibitor of indole-3-glycerol phosphate synthase with activity against multidrug-resistant *Mycobacterium tuberculosis*. FEBS J 2009, 276: 144–154.
28 Woehl E and Dunn MF. Mechanisms of monovalent cation action in enzyme catalysis: the tryptophan synthase α-, β-, and αβ-reactions. Biochemistry 1999, 38: 7131–7141.
29 Hyde CC, Ahmed SA, Padlan EA, Miles EW and Davies DR. Three-dimensional structure of the tryptophan synthase $\alpha_2\beta_2$ multienzyme complex from *Salmonella typhimurium*. J Biol Chem 1988, 263: 17857–17871.
30 Banik U, Ahmed SA, McPhie P and Miles EW. Subunit assembly in the tryptophan synthase $\alpha_2\beta_2$ complex, stabilization by pyridoxal phosphate aldimine intermediates. J Biol Chem 1995, 270: 7944–7949.
31 Marabotti A, De Biase D, Tramonti A, Bettati S and Mozzarelli A. Allosteric communication of tryptophan synthase. Functional and regulatory properties of the βS178P mutant. J Biol Chem 2001, 276: 17747–17753.
32 Peracchi A, Bettati S, Mozzarelli A, Rossi GL, Miles EW and Dunn MF. Allosteric regulation of tryptophan synthase: effects of pH, temperature, and α-subunit ligands on the equilibrium distribution of pyridoxal 5′-phosphate-*L*-serine intermediates. Biochemistry 1996, 35: 1872–1880.